biomechanics

MDPI

Article

Relationship between Joint Stiffness, Limb Stiffness and Whole–Body Center of Mass Mechanical Work across Running Speeds

Li Jin [1,*] and Michael E. Hahn [2,3]

[1] Biomechanics Research Laboratory, Department of Kinesiology, San José State University, San José, CA 95192, USA
[2] Neuromechanics Laboratory, Department of Human Physiology, University of Oregon, Eugene, OR 97403, USA
[3] Bowerman Sports Science Center, Department of Human Physiology, University of Oregon, Eugene, OR 97403, USA
* Correspondence: li.jin@sjsu.edu

Abstract: The lower–extremity system acts like a spring in the running stance phase. Vertical stiffness (K_{vert}) and leg stiffness (K_{leg}) reflect the whole–body center of mass (COM) and leg–spring system loading and response in running, while joint stiffness (K_{joint}) represents joint–level dynamic loading and response. This study aimed to investigate whether K_{joint} is associated with K_{vert} and K_{leg} across different running speeds. Twenty healthy subjects were recruited into a treadmill running study (1.8 to 3.8 m/s, with 0.4 m/s intervals). We found that K_{joint} accounted for 38.4% of the variance in K_{vert} ($p = 0.046$) and 42.4% of the variance in K_{leg} ($p = 0.028$) at 1.8 m/s; K_{joint} also accounted for 49.8% of the variance in K_{vert} ($p = 0.014$) and 79.3% of the variance in K_{leg} ($p < 0.0001$) at 2.2 m/s. K_{knee} had the strongest unique association with K_{vert} and K_{leg} at 1.8 and 2.2 m/s. K_{joint} was associated with K_{leg} at a wider range of speeds. These findings built a connection between joint stiffness and limb stiffness within a certain range of running speeds. K_{knee} may need to be considered as an important factor in future limb stiffness optimization and general running performance enhancement.

Keywords: joint stiffness; leg stiffness; vertical stiffness; center of mass; mechanical work; running

Citation: Jin, L.; Hahn, M.E. Relationship between Joint Stiffness, Limb Stiffness and Whole–Body Center of Mass Mechanical Work across Running Speeds. *Biomechanics* **2022**, *2*, 441–452. https://doi.org/10.3390/biomechanics2030034

Academic Editors: Zimi Sawacha, Giuseppe Vannozzi and Andrea Merlo

Received: 29 July 2022
Accepted: 26 August 2022
Published: 30 August 2022

1. Introduction

The lower extremity is compliant during the stance phase of running [1], with the joints going through a flexion and then an extension movement [1]. These motions suggest that in response to external force, the lower extremity musculoskeletal system acts like a spring, absorbing energy in the first half of the stance and returning a portion of elastic energy in the second half of the stance [2–4]. This results in the whole–body center of mass (COM) position reaching its minimum height at mid–stance'; the movement trajectory is similar to a bouncing ball [1,3]. Using this analogy, a simplified spring–mass model has been proposed, and is widely used in the analysis of human running gait [1,5–9].

The loading and unloading characteristics of the leg spring system under external moment and force in the running stance phase can be regarded as stiffness patterns. Vertical stiffness (K_{vert}), leg stiffness (K_{leg}) and joint stiffness (K_{joint}) can be directly calculated from running activities [6]. Moreover, K_{vert} and K_{leg} can be calculated via the spring–mass model mentioned previously. K_{vert} is the peak ground reaction force (GRF) divided by the vertical COM displacement, and it reflects COM vertical movement and oscillation characteristics in the stance phase [6,10,11]; it has been reported to increase with running speeds [6,12–14]. This may be attributed to an increase in the peak vertical GRF whilst COM displacement decreases when running speeds increase [6]. K_{leg} is the peak GRF divided by the maximum leg vertical displacement during ground contact [5–7], and K_{leg}

has been reported to remain unchanged when running speeds are below 4.0 m/s, and it tends to increase at faster speeds [5–7,12,14–16]. K_{joint} is the peak joint moment divided by the peak joint flexion angular displacement, and it reflects joint–level intersegmental displacement as a function of joint moment loading [17–20]. It has been reported that K_{ankle} remains unchanged when running from slow to fast speeds (2.5–9.7 m/s), while K_{knee} increases with running speeds [21,22].

K_{vert}, K_{leg} and K_{joint} reflect different levels of loading and displacement in running: K_{vert} and K_{leg} are from the whole–body COM vertical motion, lower extremity system loading and response aspect [6,10,11], while K_{joint} is from a relatively lower level, i.e., joint dynamic loading and response [17]. Most of the previous studies were either focused on K_{vert} and K_{leg}, or K_{joint} individually. It remains the case that little is known about whether connections exist between the lower–level system stiffness (K_{ankle}, K_{knee}, K_{hip}) and higher–level system stiffness (K_{vert}, K_{leg}) in running across speeds. From the previous findings, it can be surmised that K_{vert} and K_{leg} patterns may emerge from local joint level elasticity (or stiffness) characteristics [23–26] and musculoskeletal system geometry [10,27].

At the whole–body level, COM gravitational potential energy (E_{pot}) and mechanical kinetic energy (E_{kin}) curve patterns are characterized as being in–phase during running [28]. Specifically, both E_{pot} and E_{kin} reach their minimum values at mid–stance. Furthermore, there is minimal mechanical energy exchange between E_{pot} and E_{kin} in running [1], due to similar fluctuation patterns during the stance phase [28]. Previous studies have investigated whole–body COM mechanical work (W_{com}) and power (P_{com}) in walking [29–31], the walk–to–run transition process [28], and running in a range of speeds [32,33]. However, little is known about W_{com}'s potential connection with K_{vert} and K_{leg} while running across a range of speeds. The reason to investigate the connection between W_{com} with K_{vert} and K_{leg} is that as part of the subsystem in the spring–mass model, sagittal plane COM displacement in response to GRF is dictated by stance limb spring energy absorption and generation. The COM oscillation pattern is likely to be connected with the amount of mechanical energy going through COM, also known as mechanical work. The investigation of the connections between W_{com}, K_{vert}, and K_{leg} across running speeds would be helpful in order to identify the whole–body COM, leg spring dynamic movement mechanics, and the oscillatory energetic patterns. This information will be beneficial for the improvement of running gait performance.

The primary purpose of this study was to investigate whether K_{joint} has any association with K_{vert} or K_{leg} within each running speed. Additionally, we planned to investigate whether a connection exists between sagittal plane W^{+}_{coms} and K_{vert}, W^{+}_{coms} and K_{leg} across running speeds. Moreover, we also aimed to identify whether changing running speeds will influence K_{joint}, K_{vert}, K_{leg}, W_{com} and P_{com}. The findings from this study should be helpful to provide a framework for running gait mechanics optimization, as increasing passive stiffness in the musculoskeletal system influences lower extremity stiffness, which has been reported to be related to performance enhancement [6,34,35]. Based on these concepts, we hypothesized that: (1) K_{joint} would have a significant association with K_{vert} and K_{leg} at each running speed, respectively; (2) W_{com} would have a positive association with K_{vert} and K_{leg} across running speeds, respectively; and (3) the change of running speeds will have a significant influence on K_{joint}, K_{vert}, K_{leg}, W_{com} and P_{com}.

2. Materials and Methods

2.1. Participants

Twenty healthy participants (10 males, 10 females; 36.8 ± 15.3 years, 171.6 ± 11.2 cm, 68.5 ± 14.1 kg) were enrolled in the study. All of the participants signed informed written consent approved by the university's institutional review board before participation. All of the participants were without lower extremity musculoskeletal–related injuries for the past 6 months before the test.

2.2. Experimental Protocol and Data Collection

We measured the participants' body mass, height and leg length (L_0) before the running test. Leg length (L_0) was measured as the vertical distance from the greater trochanter to the floor during static standing [9]. Then, fifty–five retro–reflective markers were placed on the skin surface of the participants, based on a previously published whole–body marker set [36]. The participants were asked to run on a force–instrumented treadmill (Bertec, Inc., Columbus, OH, USA) at six different speeds, from 1.8 to 3.8 m/s (0.4 m/s intervals), for 75 s per stage. Data were extracted from the middle strides (20 strides on average) of each stage. Segmental kinematic data were collected at 120 Hz using an 8–camera motion capture system (Motion Analysis Corp., Santa Rosa, CA, USA). Ground reaction force data were collected at 1200 Hz using the force–instrumented treadmill. Kinematic and kinetic data were filtered with a low–pass fourth–order Butterworth filter at 6 Hz and 50 Hz, respectively.

2.3. Data Analysis

The whole–body COM position (X_{com}) was calculated from the weighted sum of a 15–segment (head, trunk, pelvis, upper arms, lower arms, hands, thighs, shanks, and feet) full–body model [37] for each subject in Visual 3D (C–Motion, Inc., Germantown, MD, USA). Specifically, it was calculated as follows:

$$X_{com} = \frac{\sum_{i=1}^{n} \left(m_{seg\ i} \cdot X_{seg\ com\ i} \right)}{m_b}, \quad (1)$$

where n is the number of the segment, $m_{seg\ i}$ is each individual segment's mass, $X_{seg\ com\ i}$ is each individual segment's center of mass coordinate, and m_b is the whole–body mass.

The spring–mass model vertical stiffness (K_{vert}) was calculated from the peak vertical ground reaction force ($vGRF_{peak}$) divided by the vertical displacement of the COM from ground contact until mid–stance (Δy) (Figure 1) [2,5–9], expressed as

$$K_{vert} = \frac{vGRF_{peak}}{\Delta y}, \quad (2)$$

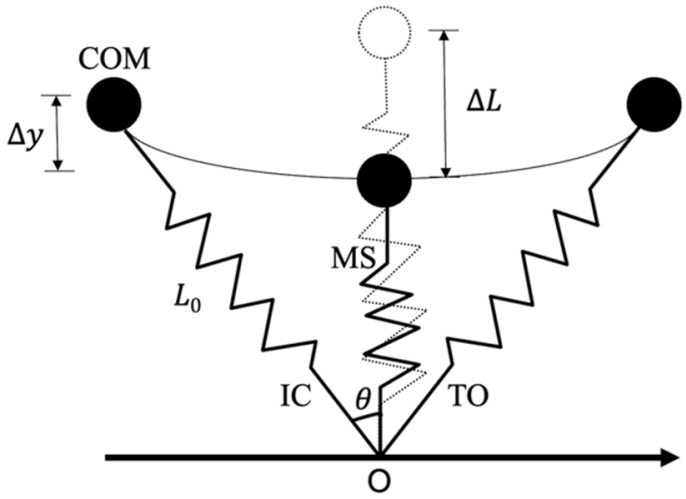

Figure 1. Schematic representative of a spring–mass model in the running stance phase. The model consists of a point mass (COM) equivalent to the body mass and the leg as a massless linear spring. The leg spring is compressed, and reaches maximum compression (ΔL) at mid–stance. The COM displacement in the vertical direction is denoted as Δy. The half swept angle of the leg spring is denoted as θ. IC: initial–contact. MS: mid–stance. TO: toe–off. Point O is the ground contact location.

The half swept angle (θ) was defined as the angle between the leg–spring at ground contact and mid–stance (Figure 1), and it was calculated from the running speed (μ), ground contact time (t_c) and initial leg length (L_0) [2,8], expressed as

$$\theta = sin^{-1}\left(\frac{\mu t_c}{2L_0}\right), \quad (3)$$

The leg–spring maximum displacement (ΔL) can be calculated via the expression of changes in the vertical COM displacement (Δy), half swept angle (θ) and initial leg length (L_0) (Figure 1) [2,5,7,9], expressed as

$$\Delta L = L_0(1 - cos\ \theta\ )\Delta y, \quad (4)$$

Leg stiffness (K_{leg}) was calculated as the peak vertical ground reaction force ($vGRF_{peak}$) divided by the leg–spring maximum displacement (ΔL) (Figure 1) [2,5–9], expressed as

$$K_{leg} = \frac{vGRF_{peak}}{\Delta L}, \quad (5)$$

Lower–extremity joint moments were calculated using a standard inverse dynamics model [38] coded in Visual 3D. In this study, each joint neutral position was defined as the zero–degree reference angle in the sagittal plane, joint extension was defined as positive, and flexion was defined as negative, in comparison with the neutral position. Joint stiffness (K_{joint}) was calculated as the change in the sagittal plane joint moment (ΔM_{joint}) divided by the sagittal plane joint angular displacement ($\Delta\theta_{joint}$) in the first half of ground contact, based on the anterior–posterior ground reaction force value [22,39], expressed as

$$K_{joint} = \frac{\Delta M_{joint}}{\Delta\theta_{joint}}, \quad (6)$$

The COM gravitational potential energy (E_{pot}) was calculated as the product of the body mass (m_b), gravitational constant (g = 9.81 m/s^2), and instantaneous COM height (h_i) [28], expressed as

$$E_{pot} = m_b g h_i, \quad (7)$$

The value of the COM kinetic energy (E_{kin}) was calculated from the sum of E_{kin} in both the horizontal and vertical direction [28], expressed as

$$E_{kin} = \frac{1}{2}(m_b v_h^2 + m_b v_v^2), \quad (8)$$

where v_h and v_v are the COM velocity in the horizontal and vertical directions, respectively. We also calculated the COM instantaneous power in the horizontal (P_{comh}) and vertical (P_{comv}) directions, and the sagittal plane (P_{coms}), based on the definition of a previous study [28], expressed as

$$P_{comh} = m_b a_h v_h, \quad (9)$$

$$P_{comv} = m_b(g + a_v)v_v, \quad (10)$$

$$P_{coms} = P_{comh} + P_{comv}, \quad (11)$$

where a_h and a_v are the COM acceleration in the horizontal and vertical directions, respectively. Moreover, the COM positive (W_{com}^+) and negative external mechanical work (W_{com}^-) in the horizontal and vertical directions, as well as in sagittal plane were calculated as the instantaneous positive (P_{com}^+) or negative power (P_{com}^-) in each direction or plane integrated over time, respectively [28].

Ground reaction force (GRF) and virtual leg length (instantaneous leg length/L_0) force–length relationships were plotted for the average of the twenty participants, for further interpretation (Figure 2). The curve slope was estimated via the tangent function

between the curve ascending phase starting point and the ascending phase ending point horizontal and vertical axis coordinate values, respectively (Figure 2). The group mean COM potential energy (E_{pot}), kinetic energy (E_{kin}) and sagittal plane COM instantaneous power (P_{coms}) were plotted from three representative speeds (1.8, 2.6, 3.8 m/s) as well (Figure 3a,b). All of the graphs were plotted in the MATLAB program (R2018a, Mathworks, Natick, MA, USA).

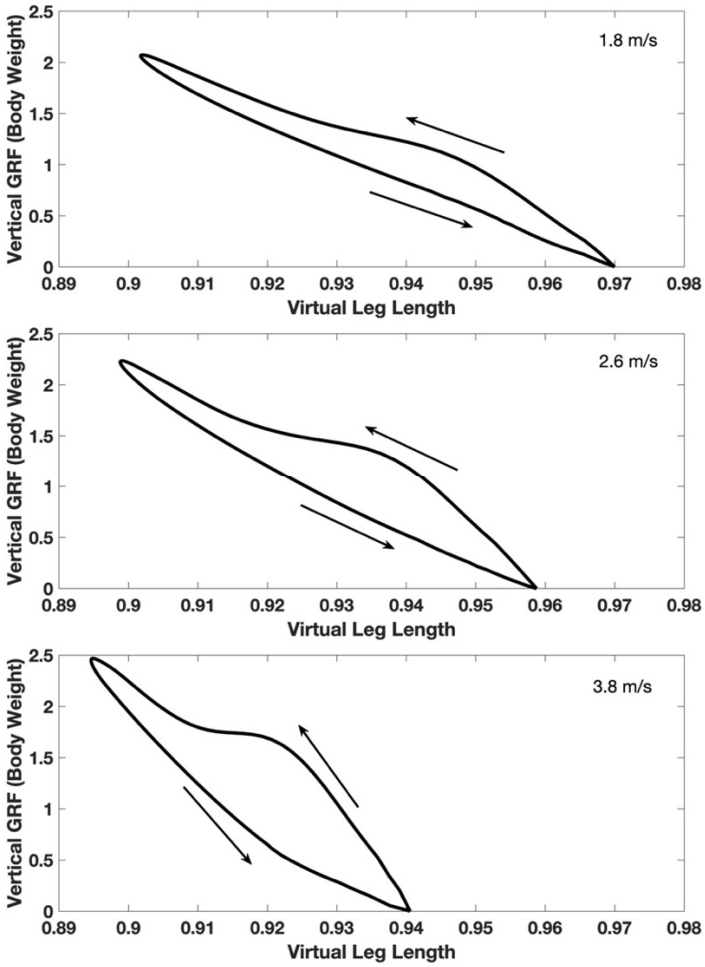

Figure 2. Group average (n = 20) leg–spring force–length curves at three representative speeds. GRF: vertical ground reaction force normalized to body weight. Virtual leg length: instantaneous leg length/L_0.

All of the outcome variables were calculated and averaged from both limbs, and were averaged across three selected gait cycles among the 20 strides for each stage. In order to make better comparisons with previous studies, only K_{joint} was normalized to body weight. The vertical stiffness (K_{vert}), leg stiffness (K_{leg}), joint stiffness (K_{joint}), COM positive work (W^{+}_{com}) and negative work (W^{-}_{com}), and COM peak positive (P^{+}_{coms}) and negative power (P^{-}_{coms}) in the sagittal plane were examined using a one–way ANOVA to compare among six speeds. The initial alpha level was set to 0.05. When the main effect was detected, Bonferroni adjustments were used for pairwise comparison, such that the alpha level was divided by the number of comparisons (adjusted $\alpha = 0.0033$ for all pairwise comparisons in this study). Additionally, multiple linear regression analysis was conducted to develop models to build potential associations between K_{joint} (ankle, knee and hip joint stiffness), K_{vert} and K_{leg} within each running speed. Lastly, simple linear regression analysis was used to examine the relationships between the sagittal plane COM positive work (W^{+}_{coms}) and K_{vert} and K_{leg} across the speeds. All of the statistical analyses were performed using SPSS (V22.0, IBM, Armonk, NY, USA).

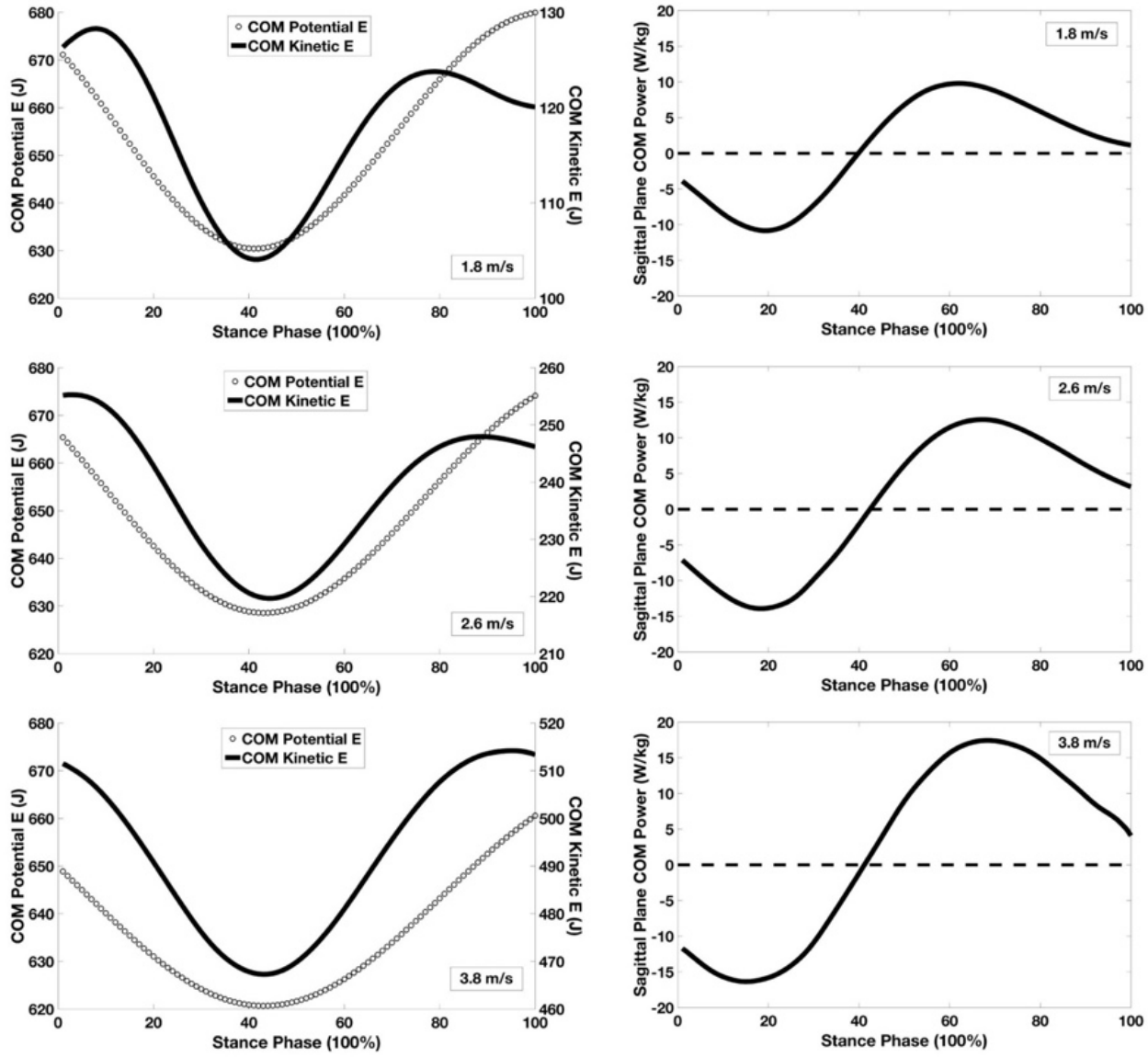

(**a**) (**b**)

Figure 3. Group average (n = 20), (**a**) whole–body COM gravitational potential energy (E_{pot}) and mechanical kinetic energy (E_{kin}) in the stance phase of three representative speeds; (**b**) sagittal plane whole–body COM instantaneous mechanical power (P_{coms}) in the stance phase of three representative speeds.

3. Results

3.1. Stiffness

The comparison of K_{leg} among all of the running speeds was not significant ($p = 0.413$). Speed's main effect for K_{vert} was significant ($p < 0.0001$), therefore, pairwise comparison was conducted (Table 1): K_{vert} at 1.8 m/s was significantly lower than all speeds between 2.6 and 3.8 m/s ($p < 0.0001$), K_{vert} at 2.2 m/s was lower than all speeds between 3.0 and 3.8 m/s ($p \leq 0.0001$), K_{vert} at 2.6 m/s was lower than at 3.4 m/s ($p = 0.001$) and 3.8 m/s ($p = 0.0002$), and K_{vert} at 3.0 m/s was lower than at 3.8 m/s ($p = 0.0032$). For K_{joint} comparison, speed's main effect was significant in K_{knee} ($p < 0.0001$), and pairwise comparison was conducted: K_{knee} at 1.8 m/s was lower than that at 3.0 m/s ($p = 0.002$) and 3.8 m/s ($p = 0.001$), and K_{knee} at 2.2 m/s was lower than that at 3.0 m/s ($p = 0.001$) and 3.8 m/s ($p = 0.003$).

Table 1. Vertical stiffness (kN/m), leg stiffness (kN/m) and joint stiffness (Nm/kg/deg) across running speeds. Sample mean (standard deviation); n = 20.

Stiffness	Running Speed (m/s)					
	1.8	**2.2**	**2.6**	**3.0**	**3.4**	**3.8**
K_{vert}	23.03 (5.19) [a]	24.98 (4.77) [b]	27.10 (4.50) [a,c]	29.79 (4.70) [a,b,d]	32.84 (6.40) [a,b,c]	40.29 (9.16) [a,b,c,d]
K_{leg}	13.49 (3.40)	13.39 (3.85)	13.22 (3.28)	13.07 (2.76)	12.96 (3.65)	13.45 (4.17)
K_{ankle}	0.18 (0.08)	0.18 (0.05)	0.19 (0.06)	0.19 (0.09)	0.21 (0.07)	0.23 (0.09)
K_{knee}	0.10 (0.02) [e]	0.11 (0.02) [f]	0.12 (0.03)	0.14 (0.04) [e,f]	0.15 (0.06)	0.18 (0.08) [e,f]
K_{hip}	0.25 (0.14)	0.22 (0.11)	0.26 (0.12)	0.24 (0.07)	0.27 (0.10)	0.27 (0.10)

[a]: Statistically significant differences of K_{vert} between 1.8 m/s and all speeds between 2.6 and 3.8 m/s, respectively ($p < 0.0001$); [b]: differences of K_{vert} between 2.2 m/s and all speeds between 3.0 and 3.8 m/s, respectively ($p \leq 0.0001$); [c]: differences of K_{vert} between 2.6 m/s and 3.4 m/s ($p = 0.001$), and 2.6 m/s and 3.8 m/s ($p = 0.0002$); [d]: differences of K_{vert} between 3.0 m/s and 3.8 m/s ($p = 0.0032$); [e]: differences of K_{knee} between 1.8 m/s and 3.0 m/s ($p = 0.002$), and 1.8 m/s and 3.8 m/s ($p = 0.001$); [f]: differences of K_{knee} between 2.2 m/s and 3.0 m/s ($p = 0.001$), and 2.2 m/s and 3.8 m/s ($p = 0.003$).

3.2. Mechanical Work and Power

Speed's main effects were significant in both W^{+}_{coms} ($p < 0.0001$) and W^{-}_{coms} ($p = 0.002$); therefore, pairwise comparison was conducted (Table 2): W^{+}_{coms} at 1.8 m/s was lower than at 3.0 m/s ($p = 0.002$), 3.4 m/s ($p < 0.0001$) and 3.8 m/s ($p = 0.003$), and the magnitude of W^{-}_{coms} at 1.8 m/s was lower than at 3.4 m/s ($p = 0.002$). Speed's main effects were also significant in both W^{+}_{comh} ($p < 0.0001$) and W^{-}_{comh} ($p < 0.0001$), and a pairwise comparison was conducted: W^{+}_{comh} at 1.8 m/s was lower than all speeds between 2.6 and 3.8 m/s ($p < 0.0003$); W^{+}_{comh} at 2.2 m/s was lower than all speeds between 3.0 and 3.8 m/s ($p < 0.002$); W^{+}_{comh} at 2.6 m/s was lower than at 3.4 m/s and 3.8 m/s, respectively ($p < 0.001$); W^{+}_{comh} at 3.0 m/s was lower than at 3.8 m/s ($p = 0.0009$); W^{-}_{comh} at 1.8 was lower than at all speeds between 2.6 and 3.8 m/s ($p < 0.0001$); and W^{-}_{comh} at 2.2 m/s was lower than at 3.4 m/s ($p = 0.0004$).

Table 2. Whole–body COM positive and negative mechanical work (J/kg) and sagittal plane *COM* peak positive and negative power (W/kg) across the speeds. Sample mean (standard deviation); n = 20.

	Running Speed (m/s)					
	1.8	**2.2**	**2.6**	**3.0**	**3.4**	**3.8**
Work						
W^{+}_{coms}	1.03 (0.14) [a]	1.06 (0.23)	1.16 (0.14)	1.21 (0.20) [a]	1.22 (0.31) [a]	1.31 (0.29) [a]
W^{-}_{coms}	−0.85 (0.11) [b]	−0.90 (0.12)	−0.96 (0.11)	−0.96 (0.13)	−0.98 (0.15) [b]	−0.94 (0.19)
W^{+}_{comh}	0.21 (0.05) [c]	0.26 (0.08) [d]	0.33 (0.09) [c,e]	0.39 (0.12) [c,d,f]	0.43 (0.17) [c,d,e]	0.54 (0.17) [c,d,e,f]
W^{-}_{comh}	−0.17 (0.05) [g]	−0.22 (0.05) [h]	−0.30 (0.08) [g]	−0.33 (0.08) [g]	−0.37 (0.09) [g,h]	−0.39 (0.12) [g]
W^{+}_{comv}	0.83 (0.14)	0.81 (0.17)	0.85 (0.12)	0.84 (0.13)	0.81 (0.16)	0.79 (0.18)
W^{-}_{comv}	−0.69 (0.11)	−0.69 (0.11)	−0.68 (0.10)	−0.65 (0.11)	−0.62 (0.10)	−0.56 (0.11)
Power						
P^{+}_{coms}	10.80 (2.63) [i]	12.42 (2.30) [i,j]	13.99 (2.74) [i,j,k]	16.43 (3.46) [i]	17.55 (2.75) [i,j,k]	18.80 (4.92) [i,j.k]
P^{-}_{coms}	−11.39 (1.97) [l]	−12.69 (2.08) [l,m]	−14.70 (3.01)	−15.48 (2.15) [l,m]	−16.56 (2.57) [l,m]	−17.75 (4.62) [l]

[a]: Statistically significant differences of W^{+}_{coms} between 1.8 m/s and 3.0 m/s ($p = 0.002$), 1.8 m/s and 3.4 m/s ($p < 0.0001$), and 1.8 m/s and 3.8 m/s ($p = 0.003$); [b]: differences of W^{-}_{coms} between 1.8 m/s and 3.4 m/s ($p = 0.002$); [c]: differences of W^{+}_{comh} between 1.8 m/s and all speeds between 2.6 and 3.8 m/s, respectively ($p < 0.0003$); [d]: differences of W^{+}_{comh} between 2.2 m/s and all speeds between 3.0 and 3.8 m/s, respectively ($p < 0.002$); [e]: differences of W^{+}_{comh} between 2.6 m/s and all speeds between 3.4 and 3.8 m/s, respectively ($p < 0.001$); [f]: differences of W^{+}_{comh} between 3.0 m/s and 3.8 m/s ($p = 0.0009$); [g]: differences of W^{-}_{comh} between 1.8 m/s and all speeds between 2.6 and 3.8 m/s, respectively ($p < 0.0001$); [h]: differences of W^{-}_{comh} between 2.2 m/s and 3.4 m/s ($p = 0.0004$); [i]: differences of P^{+}_{coms} between 1.8 m/s and all speeds between 2.2 and 3.8 m/s, respectively ($p < 0.001$); [j]: differences of P^{+}_{coms} between 2.2 m/s and 2.6 m/s, 2.2 m/s and 3.4 m/s, 2.2 m/s and 3.8 m/s ($p < 0.001$); [k]: differences of P^{+}_{coms} between 2.6 m/s and 3.4 m/s, and 2.6 m/s and 3.8 m/s ($p \leq 0.001$); [l]: differences of P^{-}_{coms} between 1.8 m/s and 2.2 m/s, and 1.8 m/s at all speeds between 3.0 and 3.8 m/s, respectively ($p \leq 0.002$); [m]: differences of P^{-}_{coms} between 2.2 m/s and 3.0 m/s, and 2.2 m/s and 3.4 m/s ($p < 0.001$).

Additionally, speed's main effects were significant in both P^{+}_{coms} and P^{-}_{coms} ($p < 0.001$), and pairwise comparison was conducted (Table 2): P^{+}_{coms} at 1.8 m/s was lower than at all speeds between 2.2 and 3.8 m/s ($p < 0.001$); P^{+}_{coms} at 2.2 m/s was lower than at 2.6, 3.4 and 3.8 m/s, respectively ($p < 0.001$); P^{+}_{coms} at 2.6 m/s was lower than at 3.4 and 3.8 m/s, respectively ($p \leq 0.001$). For P^{-}_{coms} at 1.8 m/s, it was lower than at 2.2, 3.0, 3.4 and 3.8 m/s, respectively ($p \leq 0.002$); additionally, P^{-}_{coms} at 2.2 m/s was lower than at 3.0 and 3.4 m/s, respectively ($p < 0.001$).

3.3. Multiple and Simple Linear Regression

The results from the multiple linear regression analysis showed that K_{joint} was associated with K_{vert} at 1.8 m/s and 2.2 m/s (Table 3). At 1.8 m/s, the model accounted for 38.4% of the variance in K_{vert} ($R^2 = 0.384$, $p = 0.046$), and K_{knee} had the strongest unique association with K_{vert} at this speed ($\beta = 0.509$, $p = 0.022$). At 2.2 m/s, the model accounted for 49.8% of the variance in K_{vert} ($R^2 = 0.498$, $p = 0.014$), and K_{knee} again had the strongest unique association with K_{vert} at this speed ($\beta = 0.553$, $p = 0.011$).

Table 3. Multiple linear regression models between joint stiffness and vertical stiffness (first two rows), and leg stiffness (lower four rows). Only the speed conditions with statistically significant associations are shown; n = 20.

Variable	Speed (m/s)	β_{Kankle}	β_{Kknee}	β_{Khip}	Model Summary
K_{vert}	1.8	0.246	0.509 *	0.142	$\beta_0 = 8.298$, $R^2 = 0.384$, $p = 0.046$
K_{vert}	2.2	0.040	0.553 *	0.338	$\beta_0 = 9.289$, $R^2 = 0.498$, $p = 0.014$
K_{leg}	1.8	−0.076	0.532 *	0.323	$\beta_0 = 4.815$, $R^2 = 0.424$, $p = 0.028$
K_{leg}	2.2	−0.237	0.553 *	0.526 *	$\beta_0 = 3.210$, $R^2 = 0.793$, $p < 0.0001$
K_{leg}	2.6	0.048	0.456 *	0.404	$\beta_0 = 4.512$, $R^2 = 0.399$, $p = 0.039$
K_{leg}	3.4	−0.353	0.046	0.721 *	$\beta_0 = 9.760$, $R^2 = 0.474$, $p = 0.026$

*: Statistically significant contribution of K_{joint} to predict the models; β_0: linear regression model constant (y intercept); β: standardized coefficients.

Additionally, the multiple linear regression analysis revealed that K_{joint} was associated with K_{leg} among most speeds, except at 3.0 m/s and 3.8 m/s (Table 3). At 1.8 m/s, the model accounted for 42.4% of the variance in K_{leg} ($R^2 = 0.424$, $p = 0.028$), and K_{knee} had the strongest unique association with K_{leg} ($\beta = 0.532$, $p = 0.014$). At 2.2 m/s, the model accounted for 79.3% of the variance in K_{leg} ($R^2 = 0.793$, $p < 0.0001$). For this speed, however, K_{knee} ($\beta = 0.553$, $p = 0.0004$) and K_{hip} ($\beta = 0.526$, $p = 0.001$) both had a strong unique association with K_{leg}. At 2.6 m/s, the model accounted for 39.9% of the variance in K_{leg} ($R^2 = 0.399$, $p = 0.039$), and K_{knee} had a unique association with K_{leg} ($\beta = 0.456$, $p = 0.04$). At 3.4 m/s, the model accounted for 47.4% of the variance in K_{leg} ($R^2 = 0.474$, $p = 0.026$), and K_{hip} had a strong unique association with K_{leg} ($\beta = 0.721$, $p = 0.009$).

Simple linear regression analysis showed that K_{leg} was not associated with W^{+}_{coms} across the speeds ($R^2 = 0.133$, $p = 0.477$). However, K_{vert} was positively associated with W^{+}_{coms} across the speeds ($R^2 = 0.902$, $r = 0.95$, $p = 0.004$) (Table 4).

Table 4. Simple linear regression model between vertical stiffness and whole–body COM sagittal plane positive work across the speeds; n = 20.

Variable	$\beta_{W^{+}_{coms}}$	Model Summary
K_{vert}	0.950	$\beta_0 = 0.677$, $R^2 = 0.902$, $p = 0.004$

β_0: linear regression model constant (y intercept); β: standardized coefficients.

3.4. Interpretation of Graph Patterns

Based on the stance phase ground reaction force and the virtual leg length relationship for three representative speeds, we found that the slope of the curve increased as running speeds increased (estimated curve slope value: 30 at 1.8 m/s, 38 at 2.6 m/s, 56 at 3.8 m/s),

and the virtual leg length magnitude at both initial ground contact and in the take–off phase tended to decrease (virtual leg length value: 0.97 at 1.8 m/s, 0.96 at 2.6 m/s, 0.94 at 3.8 m/s; Figure 2). The COM E_{pot} slightly decreased as the running speeds increased (initial contact phase: 670–650 J from 1.8 to 3.8 m/s; mid–stance phase: 630–620 J; take–off phase: 680–660 J), while the magnitude of E_{kin} increased dramatically when speeds increased (initial contact phase: 125–510 J from 1.8 to 3.8 m/s; mid–stance phase: 105–470 J; take–off phase: 120–513 J; Figure 3a).

4. Discussion

The primary goal of this study was to investigate whether K_{ankle}, K_{knee} and K_{hip} were associated with K_{vert} and K_{leg} using multiple linear regression models for each running speed. Additionally, we investigated whether W^{+}_{coms} was associated with K_{vert} or K_{leg} across the running speeds. The initial hypothesis that K_{joint} would be associated with K_{vert} and K_{leg} was supported. The hypothesis that W^{+}_{coms} was associated with K_{vert} and K_{leg} was partially supported.

K_{joint} was associated with both K_{vert} and K_{leg} in the multiple linear regression models at slow speeds (1.8 and 2.2 m/s) (Table 3). Furthermore, K_{knee} had a significant unique association with K_{vert} and K_{leg} at these speeds. However, K_{joint} was not associated with K_{vert} among speeds from 2.6 to 3.8 m/s. One reason may be that K_{vert} tended to increase as running speeds increased, due to the increased vertical GRF and decreased COM displacement [6]. However, the change of running speeds had mixed effects on K_{joint}. Specifically, when the running speed increased, K_{knee} tended to increase, while K_{ankle} and K_{hip} remained almost constant, and they did not have a linear relationship with the change of running speeds (Table 1). Another reason may be that K_{vert} is more related to whole–body COM bouncing and oscillation patterns [6,10,11], and K_{joint} likely has a closer relationship with leg–spring stiffness than with COM oscillation characteristics.

For multiple linear regression analysis between K_{joint} and K_{leg}, the values of K_{knee} and K_{hip} were more associated with K_{leg} (Table 3). Both K_{knee} and K_{hip} were associated with K_{leg} at 2.2 m/s. Interestingly, K_{ankle} did not have much association with K_{leg} across all of the running speeds in this study. However, K_{knee} was associated with K_{leg} among most speeds. This may be attributed to the idea that the human leg is a system comprised of multiple springs, and the sub–springs can be coordinated with each other during ground contact in running. Under similar loading conditions, the spring with the smallest stiffness will undergo the largest displacement, and this would have the most influence on the overall leg–spring system stiffness [23]. In this study, K_{knee} tended to be lower than K_{ankle} and K_{hip} across all the running speeds (Table 1). Besides having more association with K_{leg} among speeds, knee joint flexion (indicating relatively lower stiffness) could also be beneficial for elastic energy storage in the first half of the stance phase and the subsequent energy return in the second half of the stance [17,22]. The joint level stiffness is influenced by both tendon stiffness and active control of the knee muscle activation [22].

In the simple linear regression analysis, K_{vert} and W^{+}_{coms} had a strong positive association across the running speeds. This may be due to the observation that both K_{vert} and W^{+}_{coms} tended to increase with the running speed. In response to greater GRF impacts, decreasing COM sagittal plane displacement and oscillation may reduce the amount of mechanical energy being absorbed via the spring–mass system in the first half of the stance phase; this would allow for more positive mechanical work to be generated through the whole–body COM.

The other goal of the study was to examine whether a change of running speeds would affect K_{vert}, K_{leg}, W_{com} and P_{com}. The initial hypothesis was partially supported. The results showed that K_{vert} increased with the running speeds, while K_{leg} remained unchanged from 1.8 to 3.8 m/s. These findings agreed with previous findings [5–7,12–16].

Changes of speed influenced both positive and negative W_{com} in the sagittal plane and in the horizontal direction, as well as the sagittal plane peak positive and negative P_{com} (Table 2). However, changes of speed did not have significant effects on either positive

or negative W_{com} in the vertical direction. This finding can be explained by the COM E_{pot} and E_{kin} curve patterns (Figure 3a). Among the three representative running speeds, both the maximum and minimum E_{pot} values slightly decreased around 3%, from 1.8 to 3.8 m/s, while the magnitude dramatically increased around 124% for E_{kin} as the running speeds increased (Figure 3a). This indicates that changes of running speed had more effect on E_{kin} than E_{pot}. Additionally, there was a greater change of COM velocity in the horizontal direction than in the vertical direction in this speed increment running protocol, and E_{kin} was affected more by a speed change in the horizontal direction than in the vertical direction. Furthermore, GRF increased in both the vertical and horizontal directions as speeds increased, indicating that COM energy absorption was greater in the first half of the stance, and that higher speeds required more positive mechanical work generated on the COM to assist the body to move forward in the following propulsive phase. This helps explain why W^{+}_{comh} and W^{-}_{comh} increased as speeds increased.

We also investigated the vertical GRF and virtual leg length relationship in three representative speeds (Figure 2). The curve consisted of an ascending and a descending phase. The ascending phase represents the loading period, and the descending phase represents the unloading period. Within the ascending phase, the "yielding" pattern became more obvious as speeds increased. Additionally, the virtual leg length at initial contact decreased as speed increased, indicating that the leg–spring compressed more with increased speed. This would be beneficial for energy absorption as external impact forces increase, and it could also be beneficial for the reduction of COM height and E_{pot} as speed increases. Moreover, the magnitude of the virtual leg length change tended to decrease as the speed increased (Figure 2). This indicates that the leg–spring became stiffer as the running speed increased.

One limitation of this study is that the leg spring was assumed not to be compressed at initial ground contact in the spring–mass model. As speed increased, the initial leg length was less than the static standing leg length (L_0), which was used in the K_{leg} calculation. This likely affected the K_{leg} results at relatively higher speeds. Furthermore, the model used to calculate the leg–spring displacement [5] underestimated the real leg–spring displacement, and this may also affect the K_{leg} values [21,40]. However, we checked the K_{leg} and K_{vert} results with a sine–wave model [14], and they both derived similar results. Additionally, a treadmill running protocol was used in this study, with controlled locomotion speeds, and thus some individual variations may have been constrained. Another limitation is that we investigated a slow–to–medium range of running speeds. Whether the COM dynamic patterns would be different in a wider range of speeds requires further investigation.

Future studies should compare the accuracy of different models in the estimation of COM dynamic patterns during locomotion. In this study, we calculated the COM instantaneous mechanical power from kinematic variables of COM movement (COM velocity and acceleration). The method was previously shown to be reliable in the estimation of COM displacement compared with the method derived from GRF [28]. Other studies have used the dot product of GRF and COM velocity to estimate COM external mechanical power, with the COM velocity being derived from the integration of GRF in these studies [29,30,41]. Further comparison between these two methods in both walking and running across different speeds is needed.

5. Conclusions

In conclusion, when running at slow–to–medium speeds, whole–body COM positive and negative mechanical work tended to increase in the sagittal plane and in the horizontal direction. Lower–extremity joint stiffness was associated with both leg stiffness and vertical stiffness using multiple linear regression models at 1.8 m/s and 2.2 m/s. Joint stiffness was associated with leg stiffness at a wider range of running speeds compared with vertical stiffness. The knee joint was more associated with vertical stiffness and leg stiffness. Sagittal–plane COM positive work and vertical stiffness had a strong positive association when running speed increased. These findings suggest that leg–spring system stiffness

was associated with subsystem joint–level stiffness characteristics. Lastly, whole–body COM mechanical work had a strong positive association with COM oscillation patterns in the stance phase of running across different speeds. These findings build a connection between joint stiffness and limb stiffness, as well as whole–body COM mechanical work and oscillation patterns across different running speeds. The outcomes of this study may be applicable to improved designs for running–specific prostheses, and to enhancing our understanding of general running performance based on joint and limb stiffness.

Author Contributions: Conceptualization, L.J. and M.E.H.; methodology, L.J. and M.E.H.; software, L.J.; validation, L.J.; formal analysis, L.J.; investigation, L.J.; resources, M.E.H.; data curation, L.J.; writing—original draft preparation, L.J.; writing—review and editing, M.E.H.; visualization, L.J.; supervision, M.E.H.; project administration, L.J. and M.E.H.; funding acquisition, L.J. and M.E.H. All authors have read and agreed to the published version of the manuscript.

Funding: This research was funded by the Betty Foster McCue Scholarship at the University of Oregon.

Institutional Review Board Statement: This study was conducted in accordance with the Declaration of Helsinki, and was approved by the Institutional Review Board of the University of Oregon (protocol #07302015.030).

Informed Consent Statement: Informed consent was obtained from all of the subjects involved in the study.

Data Availability Statement: The data presented in this study are available on request from the corresponding author.

Acknowledgments: We would like to thank Alex Denton and Zoey Kearns for their assistance in the data processing.

Conflicts of Interest: The authors declare no conflict of interest. The funders had no role in the design of the study; in the collection, analyses, or interpretation of data; in the writing of the manuscript; or in the decision to publish the results.

References

1. Farley, C.T.; Ferris, D.P. Biomechanics of Walking and Running: Center of Mass Movements to Muscle Action. *Exerc. Sport Sci. Rev.* **1998**, *26*, 253–285. [CrossRef] [PubMed]
2. Farley, C.T.; Gonzalez, O. Leg Stiffness and in Human Stride Frequency Running. *J. Biomech.* **1996**, *29*, 181–186. [CrossRef]
3. Cavagna, G.A.; Saibene, F.; Margaria, R. Mechanical Work in Running. *J. Appl. Physiol.* **1964**, *19*, 249–256. [CrossRef] [PubMed]
4. Cavagna, G.A.; Heglund, N.C.; Taylor, C.R. Mechanical Work in Terrestrial Locomotion: Two Basic Mechanisms for Minimizing Energy Expenditure. *Am. J. Physiol-Regul. Integr. Comp. Physiol.* **1977**, *233*, R243–R261. [CrossRef]
5. McMahon, T.A.; Cheng, G.C. The Mechanics of Running: How Does Stiffness Couple with Speed? *J. Biomech.* **1990**, *23*, 65–78. [CrossRef]
6. Brughelli, M.; Cronin, J. Influence of Running Velocity on Vertical, Leg and Joint Stiffness: Modelling and Recommendations for Future Research. *Sport. Med.* **2008**, *38*, 647–657. [CrossRef]
7. Farley, C.T.; Glasheen, J.; McMahon, T.A. Running Springs: Speed and Animal Size. *J. Exp. Biol.* **1993**, *185*, 71–86. [CrossRef]
8. Ferris, D.P.; Louie, M.; Farley, C.T. Running in the Real World: Adjusting Leg Stiffness for Different Surfaces. *Proc. Biol. Sci./R. Soc.* **1998**, *265*, 989–994. [CrossRef]
9. McGowan, C.P.; Grabowski, A.M.; McDermott, W.J.; Herr, H.M.; Kram, R. Leg Stiffness of Sprinters Using Running-Specific Prostheses. *J. R. Soc. Interface* **2012**, *9*, 1975–1982. [CrossRef]
10. McMahon, T.A.; Valiant, G.; Frederick, E.C. Groucho Running. *J. Appl. Physiol.* **1987**, *62*, 2326–2337. [CrossRef]
11. Cavagna, G.; Franzetti, P.; Heglund, N.; Willems, P. The Determinants of the Step Frequency in Running, Trotting and Hopping in Man and Other Vertebrates. *J. Physiol.* **1988**, *399*, 81–92. [CrossRef] [PubMed]
12. He, J.P.; Kram, R.; McMahon, T.A. Mechanics of Running Under Simulated Low Gravity. *J. Appl. Physiol.* **1991**, *71*, 863–870. [CrossRef]
13. Cavagna, G.A. Effect of an Increase in Gravity on the Power Output and the Rebound of the Body in Human Running. *J. Exp. Biol.* **2005**, *208*, 2333–2346. [CrossRef]
14. Morin, J.B.; Dalleau, G.; Kyröläinen, H.; Jeannin, T.; Belli, A. A Simple Method for Measuring Stiffness during Running. *J. Appl. Biomech.* **2005**, *21*, 167–180. [CrossRef] [PubMed]
15. Morin, J.B.; Jeannin, T.; Chevallier, B.; Belli, A. Spring-Mass Model Characteristics during Sprint Running: Correlation with Performance and Fatigue-Induced Changes. *Int. J. Sport. Med.* **2006**, *27*, 158–165. [CrossRef]

16. Biewener, A. Scaling Body Support in Mammals: Limb Posture and Muscle Mechanics. *Science* **1989**, *245*, 45–48. [CrossRef] [PubMed]
17. Jin, L.; Hahn, M.E. Modulation of Lower Extremity Joint Stiffness, Work and Power at Different Walking and Running Speeds. *Hum. Mov. Sci.* **2018**, *58*, 1–9. [CrossRef]
18. Crenna, P.; Frigo, C. Dynamics of the Ankle Joint Analyzed through Moment-Angle Loops during Human Walking: Gender and Age Effects. *Hum. Mov. Sci.* **2011**, *30*, 1185–1198. [CrossRef]
19. Davis, R.B.; DeLuca, P.A. Gait Characterization via Dynamic Joint Stiffness. *Gait Posture* **1996**, *4*, 224–231. [CrossRef]
20. Gabriel, R.C.; Abrantes, J.; Granata, K.; Bulas-Cruz, J.; Melo-Pinto, P.; Filipe, V. Dynamic Joint Stiffness of the Ankle during Walking: Gender-Related Differences. *Phys. Ther. Sport* **2008**, *9*, 16–24. [CrossRef]
21. Arampatzis, A.; Bruk, G.-P.; Metzler, V. The Effect of Speed on Leg Stiffness and Joint Kinetics in Human Running. *J. Biomech.* **1999**, *32*, 1349–1353. [CrossRef]
22. Kuitunen, S.; Komi, P.V.; Kyröläinen, H.; Kyrolainen, H. Knee and Ankle Joint Stiffness in Sprint Running. *Med. Sci. Sport. Exerc.* **2002**, *34*, 166–173. [CrossRef] [PubMed]
23. Farley, C.T.; Morgenroth, D.C. Leg Stiffness Primarily Depends on Ankle Stiffness during Human Hopping. *J. Biomech.* **1999**, *32*, 267–273. [CrossRef]
24. Günther, M.; Blickhan, R. Joint Stiffness of the Ankle and the Knee in Running. *J. Biomech.* **2002**, *35*, 1459–1474. [CrossRef]
25. Farley, C.T.; Houdijk, H.H.; Van Strien, C.; Louie, M. Mechanism of Leg Stiffness Adjustment for Hopping on Surfaces of Different Stiffnesses. *J. Appl. Physiol.* **1998**, *85*, 1044–1055. [CrossRef] [PubMed]
26. Sholukha, V.; Gunther, M.; Blickhan, R. Running Synthesis with a Passive Support Leg. In Proceedings of the XIIth International Biomechanics Seminar on Dynamical Simulation, Gothenburg, Sweden, 10–11 September 1999; pp. 63–72.
27. Greene, P.R.; McMahon, T.A. Reflex Stiffness of Man's Anti-Gravity Muscles during Kneebends While Carrying Extra Weights. *J. Biomech.* **1979**, *12*, 881–891. [CrossRef]
28. Segers, V.; Aerts, P.; Lenoir, M.; De Clercq, D. Dynamics of the Body Centre of Mass during Actual Acceleration across Transition Speed. *J. Exp. Biol.* **2007**, *210*, 578–585. [CrossRef]
29. Zelik, K.E.; Kuo, A.D. Human Walking Isn't All Hard Work: Evidence of Soft Tissue Contributions to Energy Dissipation and Return. *J. Exp. Biol.* **2010**, *213*, 4257–4264. [CrossRef]
30. Donelan, J.M.M.; Kram, R.; Kuo, A.D. Simultaneous Positive and Negative External Mechanical Work in Human Walking. *J. Biomech.* **2002**, *35*, 117–124. [CrossRef]
31. Adamczyk, P.G.; Kuo, A.D. Redirection of Center-of-Mass Velocity during the Step-to-Step Transition of Human Walking. *J. Exp. Biol.* **2009**, *212*, 2668–2678. [CrossRef]
32. Arampatzis, A.; Knicker, A.; Metzler, V.; Brüggemann, G.-P. Mechanical Power in Running: A Comparison of Different Approaches. *J. Biomech.* **2000**, *33*, 457–463. [CrossRef]
33. Fukunaga, T.; Matsuo, A.; Yuasa, K.; Fujimatsu, H.; Asahina, K. Effect of Running Velocity on External Mechanical Power Output. *Ergonomics* **1980**, *23*, 123–136. [CrossRef] [PubMed]
34. Lindstedt, S.L.; Reich, T.E.; Keim, P.; LaStayo, P.C. Do Muscles Function as Adaptable Locomotor Springs? *J. Exp. Biol.* **2002**, *205*, 2211–2216. [CrossRef] [PubMed]
35. Reich, T.E.; Lindstedt, S.L.; LaStayo, P.C.; Pierotti, D.J. Is the Spring Quality of Muscle Plastic? *Am. J. Physiol. Regul. Integr. Comp. Physiol.* **2000**, *278*, R1661–R1666. [CrossRef]
36. Sawers, A.; Hahn, M.E. Regulation of Whole-Body Frontal Plane Balance Varies within a Step during Unperturbed Walking. *Gait Posture* **2012**, *36*, 322–324. [CrossRef]
37. Resseguie, S.C.; Jin, L.; Hahn, M.E. Analysis of Dynamic Balance Control in Transtibial Amputees with Use of a Powered Prosthetic Foot. *Biomed. Eng. Appl. Basis Commun.* **2016**, *28*, 1650011. [CrossRef]
38. Winter, D.A. *Biomechanics and Motor Control of Human Movement*, 4th ed.; John Wiley & Sons: Hoboken, NJ, USA, 2009; ISBN 9780470549148.
39. Hobara, H.; Baum, B.S.; Kwon, H.J.; Miller, R.H.; Ogata, T.; Kim, Y.H.; Shim, J.K. Amputee Locomotion: Spring-like Leg Behavior and Stiffness Regulation Using Running-Specific Prostheses. *J. Biomech.* **2013**, *46*, 2483–2489. [CrossRef]
40. Blum, Y.; Lipfert, S.W.; Seyfarth, A. Effective Leg Stiffness in Running. *J. Biomech.* **2009**, *42*, 2400–2405. [CrossRef]
41. Cavagna, G.A. Force Platforms as Ergometers. *J. Appl. Physiol.* **1975**, *39*, 174–179. [CrossRef]